AD-A249 502

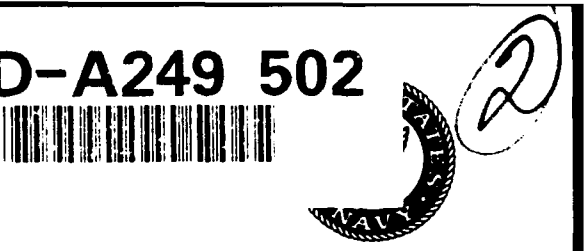

Naval Research Laboratory

Washington, DC 20375-5000

NRL/MR/4790—92-6949

Interaction of Ultra-High Laser Fields with Beams and Plasmas

ERIC ESAREY AND PHILLIP SRANGLE

Beam Physics Branch
Plasma Physics Division

April 29, 1992

DTIC
ELECTE
APR 30 1992
S B D

92-11694

Approved for public release; distribution unlimited.

92 4 28 298

REPORT DOCUMENTATION PAGE

Form Approved
OMB No 0704-0188

Public reporting burden for this collection of information is estimated to average 1 hour per response, including the time for reviewing instructions, searching existing data sources, gathering and maintaining the data needed, and completing and reviewing the collection of information. Send comments regarding this burden estimate or any other aspect of this collection of information, including suggestions for reducing this burden to Washington Headquarters Services, Directorate for Information Operations and Reports, 1215 Jefferson Davis Highway, Suite 1204, Arlington, VA 22202-4302, and to the Office of Management and Budget, Paperwork Reduction Project (0704-0188) Washington, DC 20503

1. AGENCY USE ONLY (Leave blank)	2. REPORT DATE	3. REPORT TYPE AND DATES COVERED
	April 29, 1992	Interim

4. TITLE AND SUBTITLE
Interaction of Ultra-High Laser Fields with Beams and Plasmas

5. FUNDING NUMBERS
C — AIO5-83ER401117

6. AUTHOR(S)
Eric Esarey and Phillip Sprangle

7. PERFORMING ORGANIZATION NAME(S) AND ADDRESS(ES)
Naval Research Laboratory
Washington, DC 20375-5000

8. PERFORMING ORGANIZATION REPORT NUMBER
NRL/MR/4790—92-6949

9. SPONSORING/MONITORING AGENCY NAME(S) AND ADDRESS(ES)
Department of Energy
Washington, DC 20545

10. SPONSORING/MONITORING AGENCY REPORT NUMBER

11. SUPPLEMENTARY NOTES

12a. DISTRIBUTION/AVAILABILITY STATEMENT
Approved for public release; distribution unlimited.

12b. DISTRIBUTION CODE

13. ABSTRACT *(Maximum 200 words)*

The nonlinear interaction of ultra-intense laser pulses with electron beams and plasmas is rich in a wide variety of new phenomena. Advances in laser science have made possible compact terawatt lasers capable of generating subpicosecond pulses at ultra-high powers (≥ 1 TW) and intensities ($\geq 10^{18}$ W/cm^2). These ultra-high intensities result in highly relativistic nonlinear electron dynamics. This paper briefly addresses a number of phenomena including (i) laser excitation of large amplitude plasma waves (wakefields), (ii) relativistic optical guiding of laser pulses in plasmas, (iii) optical guiding by preformed plasma channels, (iv) laser frequency amplification by ionization fronts and plasma waves, (v) relativistic harmonic generation, (vi) stimulated back-scattering from plasmas and electron beams, (vii) nonlinear Thomson scattering from plasmas and electron beams, and (viii) cooling of electron beams by intense lasers. Potential applications of these effects are also discussed.

14. SUBJECT TERMS	15. NUMBER OF PAGES
Laser plasma interactions Ultra-high laser fileds	34
	16. PRICE CODE

17. SECURITY CLASSIFICATION OF REPORT	18. SECURITY CLASSIFICATION OF THIS PAGE	19. SECURITY CLASSIFICATION OF ABSTRACT	20. LIMITATION OF ABSTRACT
UNCLASSIFIED	UNCLASSIFIED	UNCLASSIFIED	SAR

NSN 7540-01-280-5500

Standard Form 298 (Rev 2-89)
Prescribed by ANSI Std 239-18
298-102

CONTENTS

Accession For
NTIS GRA&I ☑
DTIC TAB ☐
Unannounced ☐
Justification
By
Distribution/
Availability Codes
Dist | Avail and/or Special
A-1

INTERACTION OF ULTRA-HIGH LASER FIELDS WITH BEAMS AND PLASMAS

I. INTRODUCTION

Advances in laser technology have made possible compact terawatt laser systems with high intensities ($\geq 10^{18}$ W/cm^2) modest energies (≤ 100 J) and short pulses (≤ 1 psec).[1,2] This new class of lasers is referred to as T^3 (Table-Top-Terawatt) lasers. The availability of T^3 lasers has made possible experiments in a new ultra–high intensity regime. Previous laser interaction studies have been limited, for the most part, to relatively modest intensities. At ultra–high intensities, the laser–electron interaction becomes highly nonlinear and relativistic, thus resulting in a wide variety of new and interesting phenomena.[3–18] These phenomena include: (i) laser excitation of large amplitude plasma waves (wakefields),[3–5] (ii) relativistic optical guiding of laser pulses by plasmas,[5–7] (iii) optical guiding by preformed plasma channels,[8] (iv) laser frequency amplification by ionization fronts or plasma waves,[5,9–13] (v) relativistic harmonic generation,[5,14] (vi) stimulated backscattering from plasmas and electron beams,[17] (vii) nonlinear Thomson scattering from plasmas and electron beams,[18] and (viii) the cooling of electron beams by intense lasers.[18] These phenomena may have important applications ranging from advanced ultra–high gradient accelerators to advanced sources of ultra–short wavelength coherent radiation. This paper briefly discusses some of the salient features of these phenomena.

An important parameter in the discussion of ultra–intense laser interactions is the laser strength parameter, a_0, where $a_0 = eA_0/m_0c^2$ is the normalized (unitless) peak amplitude of the laser vector potential, A_0. The laser strength parameter is related to the power, P_0, of a linearly polarized laser by

$$P_0[\mathrm{GW}] = 21.5\,(a_0 r_0/\lambda_0)^2\,, \tag{1}$$

where r_0 is the spot size of the Gaussian profile, λ_0 is the laser wavelength, and the power is in units of GW. Physically, $a_0 \geq 1$ implies that the electron quiver motion in the laser field is highly relativistic and nonlinear. This may be seen from conservation of canonical transverse momentum. In the 1D limit $a_0 = \gamma\beta_\perp$, where γ is the relativistic factor and $\beta_\perp = v_\perp/c$ is the electron quiver velocity. Hence, $a_0 \gg 1$ implies $\gamma \gg 1$. The peak laser electric field amplitude, E_0, is related to the laser strength parameter a_0 by

$$E_0[\mathrm{MeV/m}] \simeq 3 \times 10^6 a_0/\lambda_0[\mu\mathrm{m}]. \tag{2}$$

Manuscript approved March 6, 1992.

For $\lambda_0 = 1$ μm and $a_0 \geq 1$, the laser electric field exceeds the Coulomb field associated with the hydrogen atom. In terms of the laser intensity, $I_0 = 2P_0/\pi r_0^2$, the quantity a_0 is given by

$$a_0 = 0.85 \times 10^{-9} \lambda_0[\mu\text{m}] I_0^{1/2}[\text{W/cm}^2], \tag{3}$$

where λ_0 is in units of μm and I_0 is in units of W/cm^2. Highly relativistic electron motion ($a_0 \geq 1$) requires laser intensities greater than 10^{18} W/cm^2 for wavelengths of $\lambda_0 \sim 1$ μm. Such intensities are now available from compact, T^3 laser systems.

A. Compact Terawatt Lasers

The T^3 laser system is based on the technique of chirped–pulse amplification (CPA), first applied to solid–state lasers in 1985.[1] The CPA technique allows for ultra–short ($\tau_L \leq$ 1 ps) pulses to be efficiently amplified in solid–state media, such as Nd:glass, Ti:sapphire and alexandrite.[1,2] In the T^3 laser, a low energy pulse from an ultra–short pulse, mode–locked oscillator is passed through an optical fiber to produce a linear frequency chirp. The linear frequency chirp allows the pulse to be temporally stretched by a pair of gratings. The stretched pulse is amplified to moderate energies in the solid–state regenerative and single pass amplifiers. The amplified pulse is now compressed by a second matched pair of gratings. Compression of the chirped, long duration pulse is accomplished after it has been amplified, thus avoiding undesirable high field effects, e.g., self–focusing, in the solid–state medium. The CPA method is schematically shown in Fig. 1. This method has been applied to compact systems (T^3 lasers) to produce picosecond pulses in the 1-10 TW range.[1,2] Efforts are also underway to apply the CPA method to large scale systems with the goal of producing laser pulses of extremely high energies ($>$ 100 J) and powers ($>$ 100 TW).[19] In an alternative technology, large–scale KrF excimer lasers systems can directly amplify a single short pulse to terawatt power levels.[20]

II. INTENSE LASER INTERACTION PHENOMENA

A. Laser Wakefield Excitation

As an intense laser pulse propagates through an underdense plasma, $\lambda_0^2/\lambda_p^2 \ll 1$, where $\lambda_p = 2\pi c/\omega_p$ is the plasma wavelength, $\omega_p = (4\pi e^2 n_0/m_0)^{1/2}$ is the plasma frequency and n_0 is the ambient electron density, the ponderomotive force associated with the laser pulse envelope, $F_p \sim \nabla a^2$, expels electrons from the region of the laser pulse. If the pulse length, $c\tau_L$, is approximately equal to the plasma wavelength, $c\tau_L \simeq \lambda_p$, the ponderomotive force excites large amplitude plasma waves (wakefields) with phase velocities equal to the laser pulse group velocity[3-5] (see Fig. 2). The maximum wakefield amplitude generated by a linearly polarized laser pulse of amplitude a_0, in the 1D limit $r_0^2 \gg \lambda_p^2$, is[5]

$$E_{max}\,[\mathrm{GeV/m}] \simeq 3.8 \times 10^{-8} \left(n_0\,[\mathrm{cm}^{-3}]\right)^{1/2} \frac{a_0^2}{(1 + a_0^2/2)^{1/2}}, \tag{4}$$

where the maximum gradient, E_{max}, is in GeV/m and the plasma density, n_0, is in cm^{-3}. Typically, E_{max} is a few orders of magnitude greater than the accelerating gradients in conventional linear accelerators. The accelerating gradient associated with the wakefield can accelerate a trailing electron beam, i.e., such as in the laser wakefield accelerator (LWFA) shown in Fig. 2. In the absence of optical guiding, the interaction distance, L_{int}, will be limited by diffraction. Diffraction limits the interaction distance to $L_{int} \simeq \pi Z_R$, where $Z_R = \pi r_0^2/\lambda_0$ is the vacuum Rayleigh length. The maximum energy gain of the electron beam in a single stage is $\Delta W \simeq E_{max} L_{int}$ which, in the limit $a_0^2 \ll 1$, may be written as

$$\Delta W[\mathrm{MeV}] \simeq 580(\lambda_0/\lambda_p) P_0[\mathrm{TW}]. \tag{5}$$

As an example, consider a $\tau_L = 1$ psec linearly polarized laser pulse with $P_0 = 10$ TW, $\lambda_0 = 1$ μm and $r_0 = 30$ μm ($a_0 = 0.72$). The requirement that $c\tau_L \simeq \lambda_p$ implies a plasma density of $n_0 = 1.2 \times 10^{16}$ cm^{-3}. The wakefield amplitude (accelerating gradient) is $E_{max} = 2.0$ GeV/m and the interaction length is $L_{int} = 0.9$ cm. Hence, a properly phased tailing electron bunch would gain an energy of $\Delta W = 18$ MeV. The interaction length, and consequently the electron energy gain, may be greatly increased by optically guiding[5-8] the laser pulse in the plasma.

The self–consistent evolution of the nonlinear plasma wave has been studied numerically in the 1D limit.[5] Figure 3 shows the plasma density variation $\delta n/n_0 = n/n_0 - 1$ and the corresponding axial electric field E_z for a laser pulse envelope with $c\tau_L = \lambda_p$. In this figure $c\tau_L = \lambda_p = 0.03$ cm, $\lambda_0 = 10$ μm, and $a_0 = 2.0$. The steepening of the electric field and the increase in the period of the wakefield are apparent for the highly nonlinear situation shown in Fig. 3.

B. Relativistic Optical Guiding

For a laser pulse to propagate in a plasma beyond the limits of vacuum diffraction, i.e., distances large compared to Z_R, some form of optical guiding is necessary. For sufficiently powerful, long laser pulses, diffraction can be overcome by relativistic effects and the laser pulse can be optically guided in the plasma.[5–7] A nonlinear analysis of intense laser pulse propagation in underdense plasmas indicates that the index of refraction, η_R, characterizing the laser pulse evolution is given by[5]

$$\eta_R \simeq 1 - \frac{\lambda_0^2}{2\lambda_p^2}\frac{n}{\gamma n_0}, \tag{6}$$

where n is the perturbed electron density. For a long pulse laser (long rise time), $c\tau_L \gg \lambda_p$, it may be shown[5] that $n/\gamma n_0 \simeq (1+a_0^2/2)^{-1/2}$. A necessary requirement for optical guiding is that the refractive index have a maximum on axis, $\partial\eta_R/\partial r < 0$. This is the case for a long laser pulse with an intensity profile peaked on axis, $\partial a_0^2/\partial r < 0$. Analysis of the wave equation with the index of refraction given by Eq. (6) indicates that the main body of a long laser pulse will be optically guided provided the laser power, P_0, exceeds a critical threshold, $P_0 > P_{crit}$, where[6,7]

$$P_{crit}\,[\mathrm{GW}] \simeq 17.4(\lambda_p/\lambda_0)^2. \tag{7}$$

As an example, for a plasma of density $n_0 = 5 \times 10^{19}$ cm^{-3} ($\lambda_p = 20$ μm) and laser wavelength of $\lambda_0 = 1$ μm, the critical laser power is $P_{crit} = 1.36$ TW. For sufficiently short pulses, $\tau_L < 1/\omega_p$, the plasma has insufficient time to respond to the laser pulse. The modification of the refractive index occurs on the plasma frequency time scale, not on

the laser frequency time scale. Therefore, if the laser pulse duration is comparable to or shorter than a plasma period, i.e., $\tau_L \lesssim 1/\omega_p$, relativistic optical guiding does not occur.[5]

C. Optical Guiding by Density Channels

To optically guide short intense laser pulses in plasmas, preformed plasma density channels can be used.[8] Conventional optical light pipes consist of fibers having an index of refraction which varies as the square of the radial position. Optical light guides can be formed within a plasma by creating a hollow density channel. The plasma channel can be formed by propagating either a low current electron beam or a low intensity laser pulse through the plasma. In either case the plasma is expelled by the beam, leaving a density depression which cam guide the laser pulse. The plasma channel modifies the index of refraction which, in the absence of relativistic effects, is given by

$$\eta_R \simeq 1 - \frac{\lambda_0^2}{2\lambda_p^2}\frac{n(r)}{n_0}, \tag{8}$$

where $n(r)$ is the electron density profile. Optical guiding can occur when the plasma density is minimum on axis. Analysis of the wave equation for a fixed parabolic plasma density channel indicates that optical guiding of a Gaussian laser pulse occurs when the channel density depth is given by[8]

$$\Delta n = \frac{1}{\pi r_e r_0^2}, \tag{9}$$

where $\Delta n = n(r_0) - n(0)$ and $r_e = e^2/m_0c^2$ is the classical electron radius (see Fig. 4). For example, the density depression necessary to guide an optical beam having a spot size of $r_0 = 30$ μm is $\Delta n \simeq 10^{17}$ cm^{-3}. Fully nonlinear simulations of pulse propagation, which include the self-consistent evolution of the density channel, indicate that this mechanism is capable of overcoming diffraction for short pulse lengths and high intensities.[8]

The self-consistent, 2D-axisymmetric propagation of intense laser pulses in plasmas have been recently analyzed theoretically and numerically.[8] Figures 5a,b show the normalized laser intensity, a^2, as a function of $\xi = z - ct$ and r. These figures show the intensity initially, at $z = 0$, and after propagating 10 Rayleigh lengths in a preformed plasma channel. Figure 6a shows the laser spot size after 10 Rayleigh lengths. The front of the laser

pulse is optically guided while the body of the pulse focused. Figure 6b shows the evolution of the spot size as a function of propagation distance. The spot size oscillates about its initial value during the full propagation distance. In addition, as the pulse propagates within the plasma channel it generates a large amplitude wakefield. The accelerating gradient remained at a relatively constant value of $E_{max} \simeq 3$ GeV/m.

D. Laser Frequency Amplifications

A laser pulse which copropagates with an electron density wave, i.e., a traveling density gradient, can continuously change its frequency.[5,9-12] The traveling electron density gradient can be a large amplitude wakefield[9,10] or a relativistic ionization front.[5,11,12] Consider a laser pulse copropagating with a traveling density gradient which may be locally approximated by $dn/d\xi = -n_0/d$, where $\xi = z - ct$, d is the length of the density gradient and $d > c\tau_L$ is assumed, as shown in Fig. 7a. The local phase velocity is given approximately by

$$\frac{v_p(\xi)}{c} \simeq 1 + \frac{\lambda_0^2}{2\lambda_p^2}\frac{n(\xi)}{n_0}. \tag{10}$$

Hence, the phase velocity near the front of the pulse will be less than the phase velocity at the back of the pulse provided the density is less at the front of the pulse. This allows the individual phase peaks in the laser field to move closer together. This results in a decrease in the wavelength and an increase in the frequency. Analysis of the wave equation with an electron density gradient of the form $dn/d\xi = -n_0/d$ indicates that the laser frequency evolves according to[5,9-12]

$$\frac{\omega(\tau)}{\omega_0} = \left(1 + \frac{\omega_p^2}{\omega_0^2}\frac{c\tau_L}{d}\right)^{1/2}, \tag{11}$$

where $c\tau$ is the laser propagation distance. It may also be shown that the laser pulse length increases according to $\tau_L(\tau)/\tau_L(0) = \omega(\tau)/\omega_0$. Furthermore, when the density gradient is due to a large amplitude wakefield,[10] the laser strength parameter decreases as $a_0(\tau)/a_0(0) = \omega_0/\omega(\tau)$. This implies that the laser pulse gains energy from the wakefield as it propagates. However, when the density gradient is due to an externally generated ionization front,[11] the amplitude of the laser electric field decreases, $E_0(\tau)/E_0(0) = \omega_0/\omega(\tau) field.$ This implies that the laser pulse loses energy to the ionization front. Ex-

perimentally, such frequency "blue" shifts have been observed for laser pulses propagating through gases while producing self-generated ionization fronts.[12] As an example, a 0.1 ps KrF laser pulse ($\lambda_0 = 0.25$ μm) ionizing hydrogen gas at 1 atm ($\lambda_p \simeq 4.5$ μm) will double its frequency after propagating a distance of $c\tau \simeq 3.0$ cm, according to Eq. (11), assuming $d \simeq c\tau_L(0) = 30$ μm. Figure 7b shows the laser pulse profile after propagating a distance $c\tau_L = 3d\omega_0^2/\omega_p^2$ in the presence of an ionization front, as obtained from numerically solving the 1D wave equation. Notice that $\lambda(\tau) \simeq \lambda_0/2$, $E_0(\tau) \simeq E_0(0)/2$ and $\tau_L(\tau) \simeq 2\tau_L(0)$, as predicted by theory.

Alternatively, frequency amplification may be obtained by reflecting the laser pulse off a counterpropagating, relativistic ionization front.[13] In this case, the frequency of the reflected radiation will be relativistically doppler upshifted by $\omega = (1+\beta_f)^2\gamma_f^2\omega_0$, where $\beta_f = v_f/c$, $\gamma_f = (1-\beta_f^2)^{-1/2}$, and v_f is the velocity of the ionization front. Furthermore, the length of the reflected pulse will be contracted, $c\tau_L \simeq c\tau_L(0)/(1+\beta_f)\gamma_f$. However, the poor reflectivity of this relativistic "pseudo-mirror" places limitations on the applicability of this method.

E. Relativistic Harmonic Generation

The nonlinearities associated with the relativistic electron quiver motion in a linearly polarized laser field can lead to the production of harmonic radiation at odd multiples of the incident laser frequency, i.e., with wavelengths $\lambda_N = \lambda/N$, where $N = 1,3,5,....$ Coherent relativistic harmonic radiation[5,14] will be generated in the forward direction (propagating parallel to the incident laser pulse) as a result of the relativistic plasma currents driven by the incident laser pulse. Initially, the amplitude of the harmonic radiation grows linearly with the laser pulse propagation distance. Saturation of the relativistic harmonics occurs by phase detuning.[14] The nonlinear dispersion relation for a laser pulse which is long compared to the plasma wavelength, $c\tau_L \gg \lambda_p$, is given by

$$\omega^2 = c^2k^2 + \omega_p^2(1 + a_0^2/2)^{-1/2}, \tag{12}$$

where ω is the frequency, k is the wavenumber, and a linearly polarized laser pulse has been assumed in the 1D limit. Equation (12) is valid for the incident laser, $(\omega, k) = (\omega_0, k_0)$, as

well as for the harmonics, $(\omega, k) = (\omega_N, k_N)$, where $\omega_N = N\omega_0$. The detuning distance, L_d, defined to be the distance over which the relative phase between the harmonic radiation and the incident laser is equal to π, is given by $L_d|\Delta k_N| = \pi$, where $\Delta k_N = k_N(\omega_N/k_N - \omega_0/k_0)$. In the limit $\lambda_0^2/\lambda_p^2(1 + a_0^2/2)^{1/2} \ll 1$, the detuning distance is given by

$$L_d \simeq \frac{N\lambda_p^2(1 + a_0^2/2)^{1/2}}{(N^2 - 1)\lambda_0}. \tag{13}$$

At saturation, the ratio of power in the N^{th} harmonic to the incident laser power is given by[14]

$$\frac{P_N}{P_0} \simeq C_N \left(\frac{\lambda_0 a_0}{\lambda_p}\right)^{2(N-1)} \left(1 + \frac{a_0^2}{2}\right)^{-3(N-1)/2}, \tag{14}$$

where C_N are constants which decrease rapidly with increasing harmonic number, i.e., $C_3 = 4.9 \times 10^{-3}$ and $C_5 = 2.4 \times 10^{-5}$. Furthermore, driven relativistic harmonic generation is a nonresonant interaction; hence, the process is not sensitive to thermal plasma effects.

As an example, consider an incident laser with $P_0 = 10$ TW, $\lambda_0 = 1$ μm and spot size $r_0 = 10$ μm ($a_0 = 2.2$), interacting with a plasma of density $n_0 = 10^{20}$ cm^{-3} ($\lambda_p = 3.4$ μm). For the third (and fifth) harmonic, $P_N/P_0 = 2.2 \times 10^{-5}$ (4.6×10^{-10}) and $L_d = 8.0$ μm (4.3 μm). Hence, 22 MW (0.46 kW) should be observed at a wavelength of $\lambda = 3300$ Å (2000 Å). Clearly, the limitations due to phase detuning are restrictive. If a scheme for phase matching could be conceived, the interaction distance, L, and thus the harmonic power, $P_N \sim L^2$, could be increased. Furthermore, a fully ionized plasma has been assumed in which atomic and ionization effects have been neglected. Atomic[15] and ionization[16] effects may substantially enhance the amount of forward harmonic generation. This has been the case in low intensity laser interaction experiments with neutral gases, in which coherent radiation well beyond the 61^{st} harmonic has been observed.[15]

F. Stimulated backscattered harmonic generation

Stimulated backscattering[17] of intense laser pulses may occur from a stationary plasma or from a counterstreaming electron beam, i.e., a laser-pumped free-electron laser (FEL).[21] Low intensity lasers used in previous experiments resulted in the observation of only the fundamental backscattered field. At ultra-high intensities higher harmonic backscattered

radiation will be generated.[17] The frequency of the stimulated backscattered harmonic (SBH) radiation is given by $\omega = NM_0\omega_0$, where $N = 1, 3, 5...$ is the harmonic number and M_0 is the Doppler shift factor given by

$$M_0 = \begin{cases} 1, & \text{plasma}, \\ \gamma_0^2(1+\beta_0)^2/(1+a_0^2/2), & \text{e-beam}, \end{cases} \tag{15}$$

where $\gamma_0 = (1-\beta_0^2)^{-1/2}$, $\beta_0 = v_0/c$, and v_0 is the initial velocity of the counterstreaming electron beam. This is shown schematically in Fig. 8. The backscattered radiation grows exponentially from the front of the laser pulse to the back until saturation is reached. The exponential growth rate Γ of the N^{th} harmonic is found to be[17]

$$\Gamma = \sqrt{3}\left[\frac{\rho_0\omega_p^2\omega_0 M_0 F_N}{\gamma_0(1+M_0)^2}\right]^{1/3}, \tag{16}$$

where $F_N = b[J_{(N-1)/2} - J_{(N+1)/2}]^2$ is the harmonic coupling function, $J = J(b)$ are Bessel functions, $b = N(a_0^2/4)/(1+a_0^2/2)$ and $\rho_0 = (1+a_0^2/2)^{-1/2}$ for a plasma and $\rho_0 = 1$ for an electron beam. For a low intensity incident laser interacting with a plasma, $a_0^2 \ll 1$, Eq. (16) reduces to the standard expression for the growth rate of the fundamental Raman backscatter instability in the strong-pump (or strongly-coupled) regime.[22] For a low intensity incident laser interacting with an electron beam, Eq. (16) gives the growth rate of the fundamental ($N = 1$) radiation of a laser-pumped FEL in the strong-pump (or high-gain Compton) regime.[21,23] The growth rates for the higher N harmonics become significant only when $a_0 \gtrsim 1$. This is shown in Fig. 9, in which $F_N^{1/3} \sim \Gamma$ is plotted as a function of $(a_0^2/4)/(1+a_0^2/2)$.

Growth of the SBH radiation continues until the radiation amplitude is sufficiently large to cause particle trapping. At saturation, the ratio of the harmonic power to that of the incident laser is found to be[17]

$$\frac{P_N}{P_0} = \left[\frac{\rho\omega_p^2(1+MI_0)}{\gamma_0\omega_0^2 M_0^{1/2}}\right]^{4/3}\frac{F_N^{1/3}}{16bJ_0^2}. \tag{17}$$

Since stimulated backscattering is a resonant process, it is sensitive to electron thermal effects, i.e., the axial electron distribution must be sufficiently cold before exponential

growth of the radiation is achieved. Specifically, the thermal velocity must satisfy[17]

$$\beta_{th} \ll \left[\frac{\rho_0 \omega_p^2 (1+M_0)}{\gamma_0 \omega_0^2 M_0^2}\right]^{1/3} \frac{F_N^{1/3}}{2\gamma_0^2 N}. \tag{18}$$

For a plasma, the thermal energy is $\Delta E_{th} = m_0 c^2 \beta_{th}^2/2$. For an electron beam with $\gamma_0 \gg 1$, the normalized energy spread is given by $\Delta\gamma_{th}/\gamma_0 = \gamma_0^2 \beta_{th}$. Note that for the fundamental ($N = 1$) in the limit $\gamma_0 \gg 1$ and $a_0^2 \ll 1$, the thermal requirement is $\Delta\gamma_{th}/\gamma_0 \ll \eta_e$, as is the case for conventional strong-pump FELs operating at the fundamental,[23] where η_e is the electronic efficiency (the ratio of backscattered radiation power to electron beam power). The usual requirement regarding FELs operating at the fundamental, $\Delta\gamma_{th}/\gamma_0 \ll \eta_e$, however, does not in general apply to harmonic generation.

Two examples of SBH generation will be discussed: one utilizing a stationary plasma and the other utilizing a relativistic electron beam. In both examples a pump laser is assumed with $\lambda_0 = 1$ μm, $I_0 = 10^{19}$ W/cm^2 ($a_0 = 2.6$) and $r_0 = 10$ μm, which implies $P_0 = 15$ TW. Consider amplification of the third, $N = 3$, (and the fifth, $N = 5$) harmonic at a wavelength of $\lambda = 3300$ Å (2000 Å) using a plasma of density $n_0 = 10^{19}$ cm^{-3}. The e-folding length is $c/\Gamma = 1.8$ μm (2.0 μm). At saturation, the ratio of the harmonic power to the pump laser power is $P_N/P_0 = 1.0 \times 10^{-4}$ (3.8×10^{-4}), i.e., $P_N = 1.5$ GW (5.8 GW). The pulse length of the SBH radiation is approximately the transit length of the pump laser pulse through the plasma. The thermal requirement on the longitudinal energy spread is $E_{th} < 77$ eV (22 eV). Plasmas with sufficiently cold longitudinal temperatures may be produced by laser-induced ionization.[24]

In the next example, SBH radiation is generated using an intense electron beam with a current of 15 A, a beam radius of 10 μm (current density of 4.8 MA/cm^2) and an energy of 250 keV ($\gamma_0 = 1.5$). Consider amplification of the third, $N = 3$, harmonic at a wavelength of $\lambda = \lambda_0/3M_0 = 2200$ Å. The e-folding length is $c/\Gamma = 31$ μm and the thermal requirement on the longitudinal energy spread is $\Delta\gamma/(\gamma_0 - 1) < 0.18\%$. At saturation, the ratio of the third harmonic power to the pump laser power is $P_N/P_0 = 1.1 \times 10^{-9}$, i.e., $P_N = 17$ kW. The electronic efficiency at saturation is $\eta_e = 0.87\%$.

This example illustrates the difficulty of generating coherent SBH radiation, given the present state of electron beam technology. In particular, the limitations on the electron

beam energy spread for realistic current densities present a serious difficulty. If the electron distribution is not sufficiently cold, however, harmonic radiation can be generated via nonlinear Thomson scattering from individual electrons.

G. Nonlinear Thomson Scattering

Nonlinear Thomson scattering of intense laser radiation may be achieved using either a dense plasma or a counterstreaming electron beam.[18] For example, nonlinear Thomson scattering of an intense laser from a counterstreaming electron beam produces synchrotron radiation in much the same manner as a static undulator magnet in a storage ring generates synchrotron radiation (see Fig. 10). An advantage in using an intense laser pulse over a static undulator is that the wavelength of the laser pulse is several orders of magnitude shorter, $\sim 10^6$, than that of the undulator. Hence, for a given electron beam energy, a laser pulse can produce significantly shorter wavelength synchrotron radiation than an undulator. In the following, some important aspects of nonlinear Thomson scattering from a stationary plasma will be discussed. Scattering from an electron beam may be described by performing the appropriate relativistic transformations on the plasma scattering results.

For low intensity lasers ($a_0^2 \ll 1$), the frequency of the scattered radiation[25] from a dense plasma ($\omega_p \gg 1/\tau_L$) is given by $\omega = \omega_0$. Since the interaction for $a_0^2 \gg 1$ is highly nonlinear, the scattered radiation contains a continuum of harmonic radiation out to the harmonic number N_{max}. The radiation will contain appreciable frequency components up to a maximum (critical) frequency, given by $\omega_{max} = N_{max}\omega_0 = 3\gamma^3 c/\rho$, where ρ is the electron's instantaneous radius of curvature and γ is the electron's relativistic factor.[26] For $a_0^2 \gg 1$, analysis of the electron orbits in the laser field shows that the maximum harmonic number is given by[18]

$$N_{max} \simeq 3a_0^3, \tag{19}$$

where a circularly polarized incident laser field has been assumed. Furthermore, for a dense plasma in the limit $a_0^2 \gg 1$, the scattered radiation is predominantly perpendicular to the incident laser, $\theta_c \simeq \pi/2$.

The total power in the scattered radiation may be calculated from the relativistic form of Larmor's formula. The ratio of scattered power to incident laser power for a circularly

polarized laser pulse interacting with a plasma of density n_0 is given by[18]

$$P/P_0 = (8\pi/3)n_0 r_e^2 c\tau_L(1+a_0^2), \tag{20}$$

where r_e is the classical electron radius. As an example, for a circularly polarized laser with $\lambda_0 = 1$ μm, $\tau_L = 1$ ps, and $a_0 = 2$, interacting with a plasma of density $n_0 = 10^{19}$ cm^{-3}, the total scattered power is given by $P/P_0 \simeq 1.0 \times 10^{-6}$. The maximum harmonic number is $N_{max} \simeq 24$, which corresponds to a minimum wavelength of $\lambda \simeq 420$ Å. The pulse length of the scattered radiation is determined by the laser–plasma interaction time.

Furthermore, extremely short–wavelength radiation may be generated by scattering an intense laser pulse off a counterstreaming electron beam. The frequency of the radiation scattered off an electron beam will be relativistically doppler shifted by M_0, Eq. (15), in addition to the harmonic factor. The scattered radiation is also well collimated within a narrow cone of angle $\theta_c \sim 1/\gamma$ in the direction of the electron beam.

H. Laser Cooling of Electron Beams

An electron beam interacting with a counterstreaming laser pulse emits incoherent radiation via nonlinear Thomson scattering, as is shown in Fig. 10. As the electron beam radiates, it is subsequently "cooled", i.e., the normalized emittance and energy spread of the electron beam is damped.[18] This is the result of the radiation reaction force which an electron experiences while emitting radiation. The normalized electron beam emittance ϵ_n will be damped according to the relation[18]

$$\epsilon_n = \epsilon_{n0}/(1+z/L_R), \tag{21}$$

where ϵ_{n0} is the initial normalized emittance, and

$$L_R[\mu\text{m}] \simeq 3.4 \times 10^6 \lambda_0^2[\mu\text{m}]/\gamma_0 a_0^2, \tag{22}$$

is the characteristic damping distance, where γ_0 is the initial energy of the electron beam and a circularly polarized laser has been assumed. The mean energy, $\bar{\gamma}$, of the electron beam also decreases, $\bar{\gamma} = \gamma_0/(1+z/L_R)$. Furthermore, it can be shown that the fractional

beam energy spread decreases, $\Delta\gamma/\bar{\gamma} = (\Delta\gamma_0/\gamma_0)/(1 + z/L_R)$, where $\Delta\gamma_0$ is the initial beam energy spread. This radiative cooling effect can be significant. As an example, consider a $\lambda_0 = 1$ μm laser with $a_0 = 10$ interacting with an electron beam of $\gamma_0 = 200$. The damping length for these parameters is $L_R \simeq 170$ μm. The energy lost by the electron beam appears in the form of synchrotron radiation.

III. CONCLUSION

An attempt has been made to briefly discuss some of the research areas which may be impacted by the development of compact ultra–intense lasers. An important measure which characterizes ultra–intense laser interaction physics is the laser strength parameter, a_0, which is proportional to the square root of the laser intensity. When this parameter is significantly greater than unity the electron dynamics become highly relativistic and nonlinear, thus resulting in a wide variety of new phenomena. This high laser field regime has not been fully analyzed. Potential applications of these phenomena include advanced accelerators, such as the laser wakefield accelerator, advanced radiation sources, such as nonlinear Thomson synchrotron sources and laser pumped FELs, as well as a laser cooling concept for electron beams. Although a number of distinct intense laser interaction phenomena have been discussed, it should be emphasized that this is only a partial list of phenomena in a research area which is rapidly growing.

Acknowledgments

The authors acknowledge useful discussions with J. Krall, G. Joyce, A. Ting, W. Mori, D. Umstadter, and G. Mourou. This work was supported by the Department of Energy and Office of Naval Research.

References

1. D. Strickland and G. Mourou, Opt. Commun. **56**, 216 (1985); P. Maine, D. Strickland, P. Bado, M. Pessot, and G. Mourou, IEEE J. Quantum Electron. **QE-24**, 398 (1988); M. Pessot, J. A. Squire, G. A. Mourou, and D. J. Harter, Opt. Lett. **14**, 797 (1989); M. Ferray, L. A. Lompre, O. Gobert, A. L'Huillier, G. Mainfray, C. Manus, and A. Sanchez, Opt. Commun. **75**, 278 (1990); C. Sauteret, D. Husson, G. Thiell, S. Seznec, S. Gary, A. Migus, and G. Mourou, Opt. Lett. **16**, 238 (1991); J. Squier, F. Salin, G. Mourou, and D. Harter, Opt. Lett. **16**, 324 (1991).
2. M. D. Perry. F. G. Patterson, and J. Weston, Opt. Lett. **15**, 1400 (1990); F. G. Patterson, R. Gonzales, and M. Perry, Opt. Lett. **16**, 1107 (1991); F. G. Patterson, and M. Perry, J. Opt. Soc. Am. B **8**, 2384 (1991).
3. T. Tajima and J. M. Dawson, Phys. Rev. Lett. **43**, 267 (1979); L. M. Gorbunov and V. I. Kirsanov, Zh. Eksp. Teor. Fiz. **93**, 509 (1987) [Sov. Phys. JETP **66**, 290 (1987)]; V. N. Tsytovich, U. DeAngelis, and R. Bingham, Comments Plasma Phys. Controlled Fusion **12**, 249 (1989); V. I. Berezhiani and I. G. Murusidze, Phys. Lett. A **148**, 338 (1990); T. C. Katsouleas, W. B. Mori, J. M. Dawson, and S. Wilks, in SPIE Conf. Proc. **1229**, ed. by E. M. Campell (SPIE, Bellingham, WA, 1990), p. 98.
4. P. Sprangle, E. Esarey, A. Ting, and G. Joyce, Appl. Phys. Lett. **53**, 2146 (1988); E. Esarey, A. Ting, P. Sprangle, and G. Joyce, Comments Plasma Phys. Controlled Fusion **12**, 191 (1989).
5. P. Sprangle, E. Esarey, and A. Ting, Phys. Rev. Lett. **64**, 2011 (1990); Phys. Rev. A **41**, 4463 (1990); A. Ting, E. Esarey, and P. Sprangle, Phys. Fluids B **2**, 1390 (1990).
6. C. Max, J. Arons and A. B. Langdon, Phys. Rev. Lett. **33**, 209 (1974); G. Schmidt and W. Horton, Comments Plasma Phys. Controlled Fusion **9**, 85 (1985); G. Z. Sun, E. Ott, Y. C. Lee, and P. Guzdar, Phys. Fluids **30**, 526 (1987); W. B. Mori, C. Joshi, J. M. Dawson, D. W. Forslund, and I. M. Kindel, Phys. Rev. Lett. **60**, 1298 (1988); P. Gibbon and A. R. Bell, Phys. Rev. Lett. **61**, 1599 (1988); C. J. McKinstrie and D. A. Russell, Phys. Rev. Lett. **61**, 2929 (1988); T. Kurki-Suonio, P. J. Morrison, and T. Tajima, Phys. Rev. A **40**, 3230 (1989); A. B. Borisov, A. V. Borovskiy, V. V. Korobkin, A. M. Prokhorov, C. K. Rhodes, and O. B. Shiryaev, Phys. Rev. Lett.

65, 1753 (1990).

7. P. Sprangle, C. M. Tang, and E. Esarey, IEEE Trans. Plasma Sci. **PS-15**, 145 (1987); E. Esarey, A. Ting, and P. Sprangle, Appl. Phys. Lett. **53**, 1266 (1988); E. Esarey and A. Ting, Phys. Rev. Lett. **65**, 1961 (1990); P. Sprangle, A. Zigler, and E. Esarey, Appl. Phys. Lett. **58**, 346 (1991).
8. P. Sprangle, E. Esarey, J. Krall, and G. Joyce, to be published.
9. S. C. Wilks, J. M. Dawson, and W. B. Mori, Phys. Rev. Lett. **61**, 337 (1988); S. C. Wilks, J. M. Dawson, W. B. Mori, T. Katsouleas, and M. E. Jones, Phys. Rev. Lett. **62**, 2600 (1989).
10. E. Esarey, A. Ting, and P. Sprangle, Phys. Rev. A **42**, 3526 (1990).
11. E. Esarey, G. Joyce, and P. Sprangle, Phys. Rev. A **44**, 3908 (1991).
12. E. Yablonovitch, Phys. Rev. A **10**, 1888 (1974); P. B. Corkum, IEEE J. Quantum Electron. **QE-21**, 216 (1985); W. M. Wood, G. Focht, and M. C. Downer, Opt. Lett. **13**, 984 (1988).
13. M. Lampe, E. Ott, and J. H. Walker, Phys. Fluids **21**, 42 (1978); H. C. Kapteyn, and M. M. Murnane, J. Opt. Soc. Am. B **8**, 1657 (1991); W. Mori, Phys. Rev. A **44**, 5118 (1991).
14. X. Liu, D. Umstadter, J. S. Coe, C. Y. Chien, E. Esarey, and P. Sprangle, in "Coherent Short Wavelength Radiation: Generation and Application," ed. by P. Bucksbaum and N. Ceglio. (Opt. Soc. Amer., Washington, DC 1991), **11**, 32; E. Esarey and P. Sprangle, to be published; W. Mori (private communication).
15. A. McPherson, G. Gibson, A. Jarah, U. Johann, T. S. Luk, F. McIntyre, K. Boyer, and C. Rhodes, J. Opt. Soc. Am. B **4**, 595 (1987); M. Ferray, A. L'Huillier, X. F. Li, L. A. Lompre', G. Mainfray, and C. Manus, J. Phys. B: At. Mol. Opt. Phys. **21**, 231 (1988); X. F. Li, A. L'Huillier, M. Ferray, L. A. Lompre', and G. Mainfray, Phys. Rev. A **39**, 5751 (1989); M. Perry, to be published.
16. F. Brunel, J. Opt. Soc. Am. B **7**, 521 (1990).
17. P. Sprangle and E. Esarey, Phys. Rev. Lett. **67**, 2021 (1991); E. Esarey and P. Sprangle, accepted by Phys. Rev. A.
18. P. Sprangle and E. Esarey, to be published.

19. Efforts are underway at Limeil, France, and Osaka, Japan.

20. T. S. Luk, A. McPherson, G. Gibson, K. Boyer, and C. K. Rhodes, Opt. Lett. **14**, 1113 (1989); S. Watanabe, A. Endoh, M. Watanabe, H. Sarukura, and K. Hata, J. Opt. Soc. Amer. B **6**, 1870 (1989).

21. R. H. Pantell, G. Soncini, and H. E. Puthoff, IEEE J. Quantum Electron. **QE-4**, 905 (1968); A. Hasegawa, K. Mima, P. Sprangle, H. H. Szu, and V. L. Granatstein, Appl. Phys. Lett. **29**, 542 (1976); P. Sprangle and A. T. Drobot, J. Appl. Phys. **50**, 2652 (1979); L. R. Elias, Phys. Rev. Lett. **42**, 977 (1979); A. Gover, C. M. Tang, and P. Sprangle, J. Appl. Phys. **53**, 124 (1982).

22. J. F. Drake, P. K. Kaw, Y. C. Lee, G. Schmidt, C. S. Liu, and M. N. Rosenbluth, Phys. Fluids **17**, 778 (1974); D. W. Forslund, J. M. Kindel, and E. L. Lindman, Phys. Fluids **18**, 1002 (1975).

23. P. Sprangle and R. A. Smith, Phys. Rev. A **21**, 293 (1980); C. Roberson and P. Sprangle, Phys. Fluids B **1**, 3 (1989).

24. P. B. Corkum, N. H. Burnett, and F. Brunel, Phys. Rev. Lett. **62**, 1259 (1989); N. H. Burnett and P. B. Corkum, J. Opt. Soc. Am. B **6**, 1195 (1989).

25. E. S. Sarachik and G. T. Schappert, Phys. Rev. D **1**, 2738 (1970).

26. J. D. Jackson, "Classical Electrodynamics", (Wiley, New York, 1975), Chap. 14.

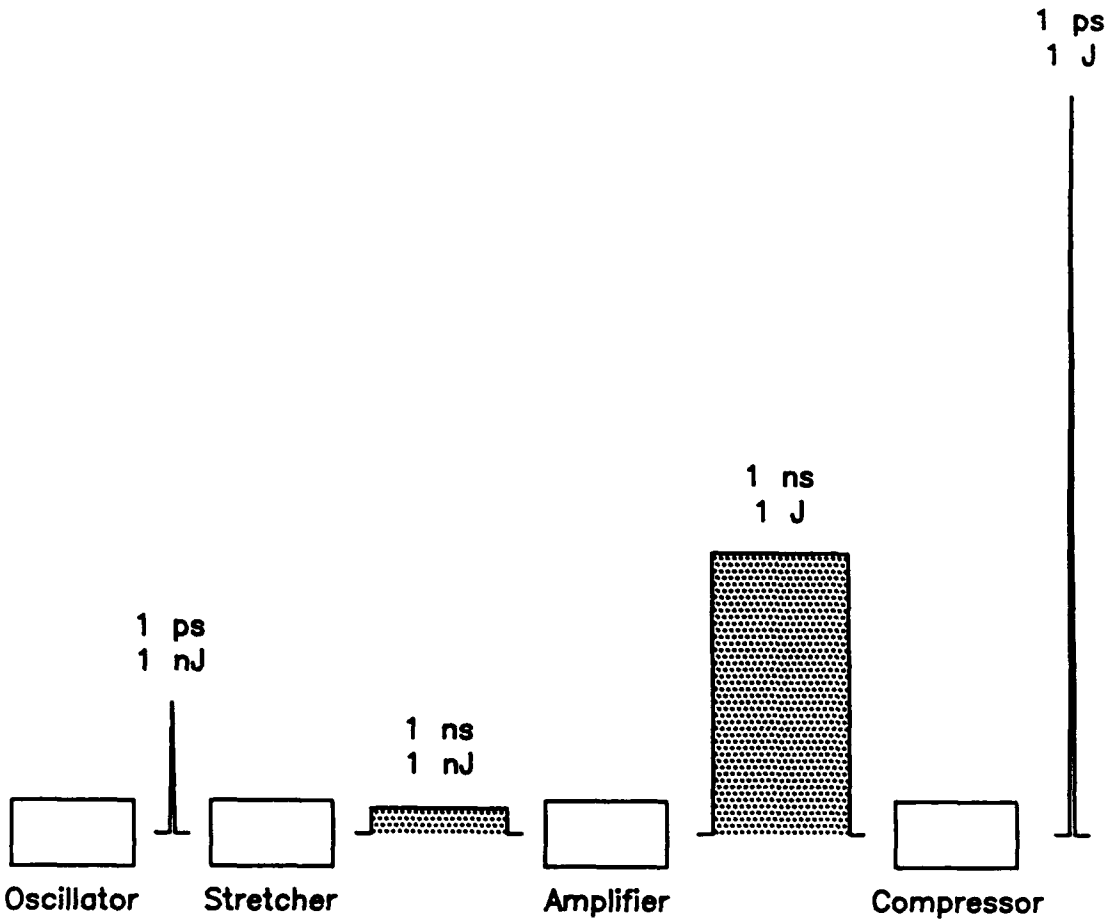

Fig. 1: Schematic of the chirped-pulse amplification (CPA) method used in T^3 laser systems.

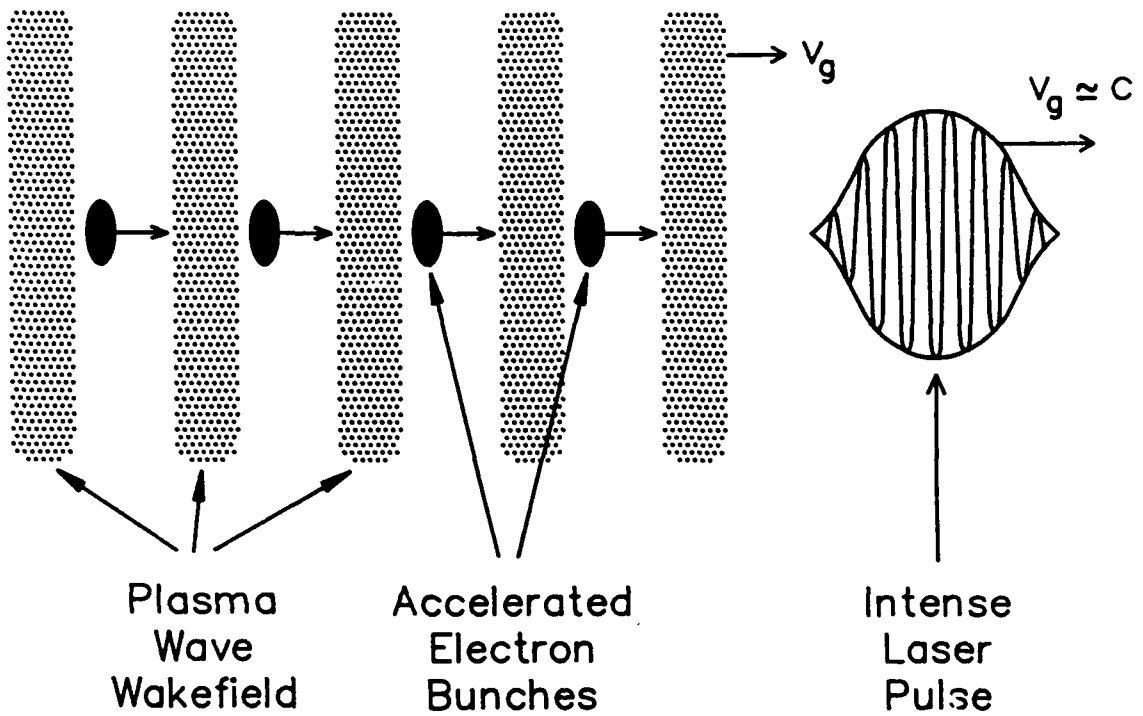

Fig. 2: Schematic of the laser wakefield accelerator (LWFA). The radiation (ponderomotive) force of an intense laser pulse drives plasma waves (wakefields) with phase velocities $\simeq c$ which trap and accelerate trailing electron bunches.

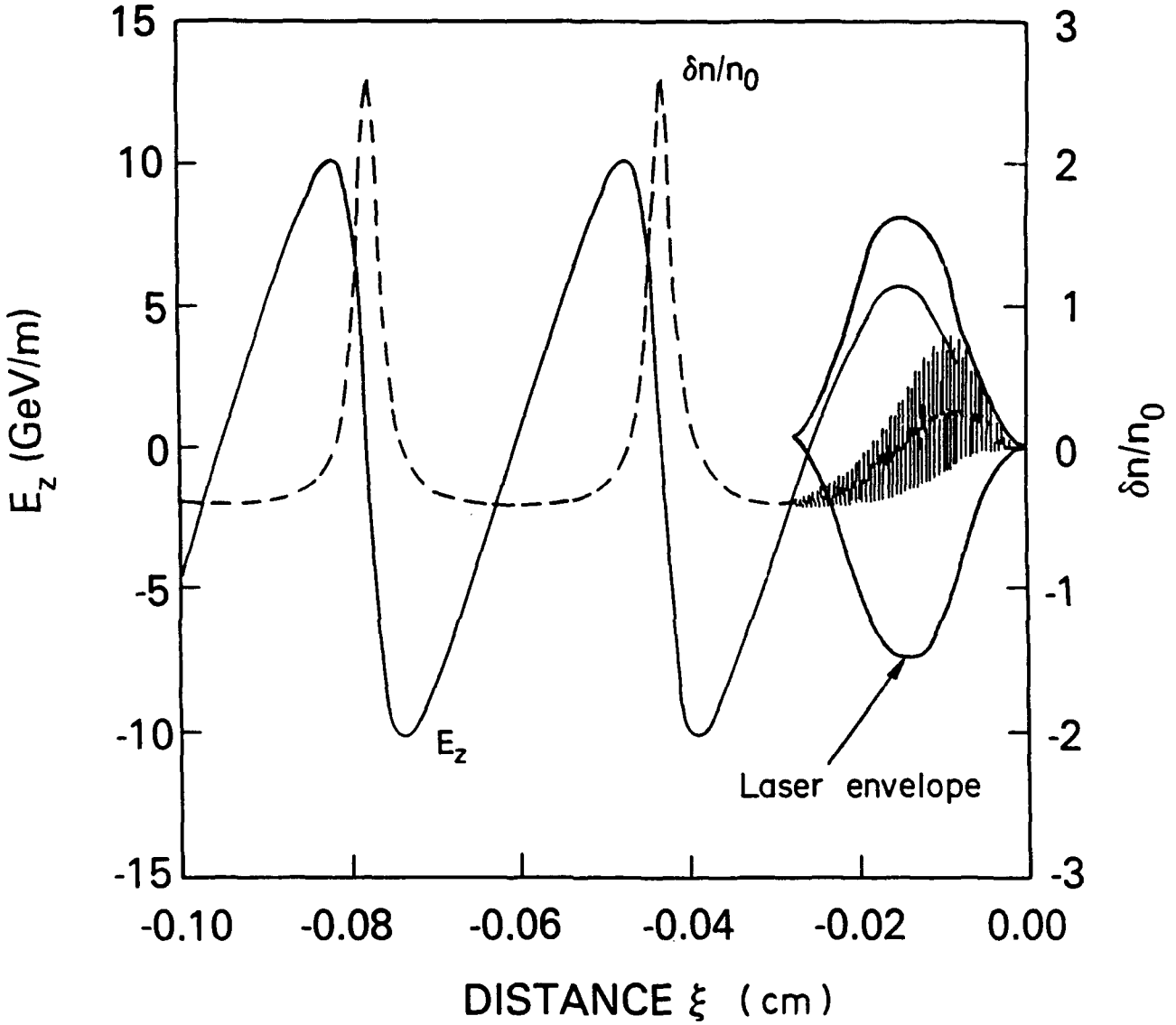

Fig. 3: Density variation $\delta n/n_0 = n/n_0 - 1$ and axial electric field E_z in GeV/m for a laser pulse with $a_0 = 2$ and $c\tau_L = \lambda_p = 0.03$ cm.

Optical Guiding in a Plasma Density Channel

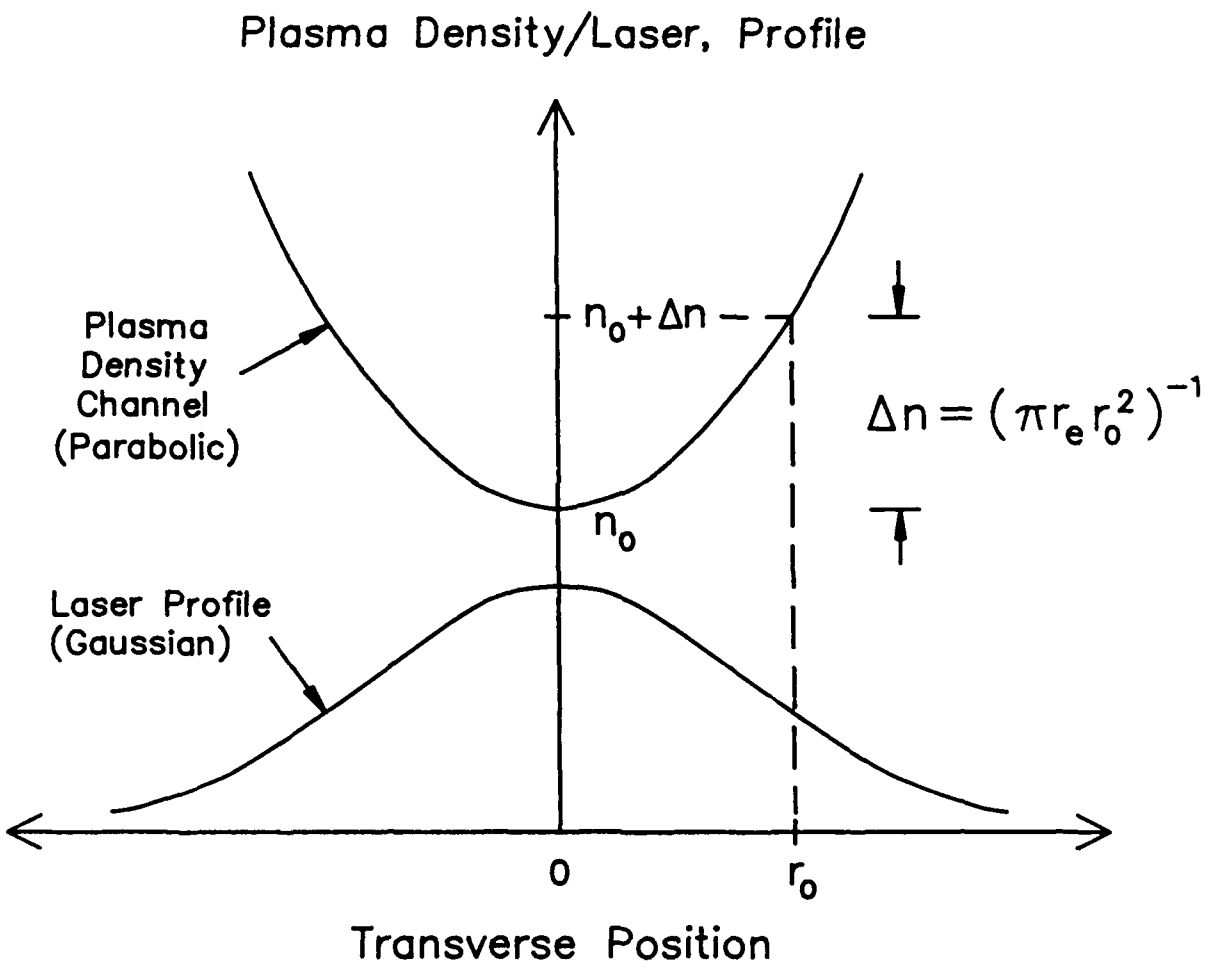

Fig. 4: Plasma channel profile necessary for optical guiding in a preformed plasma channel.

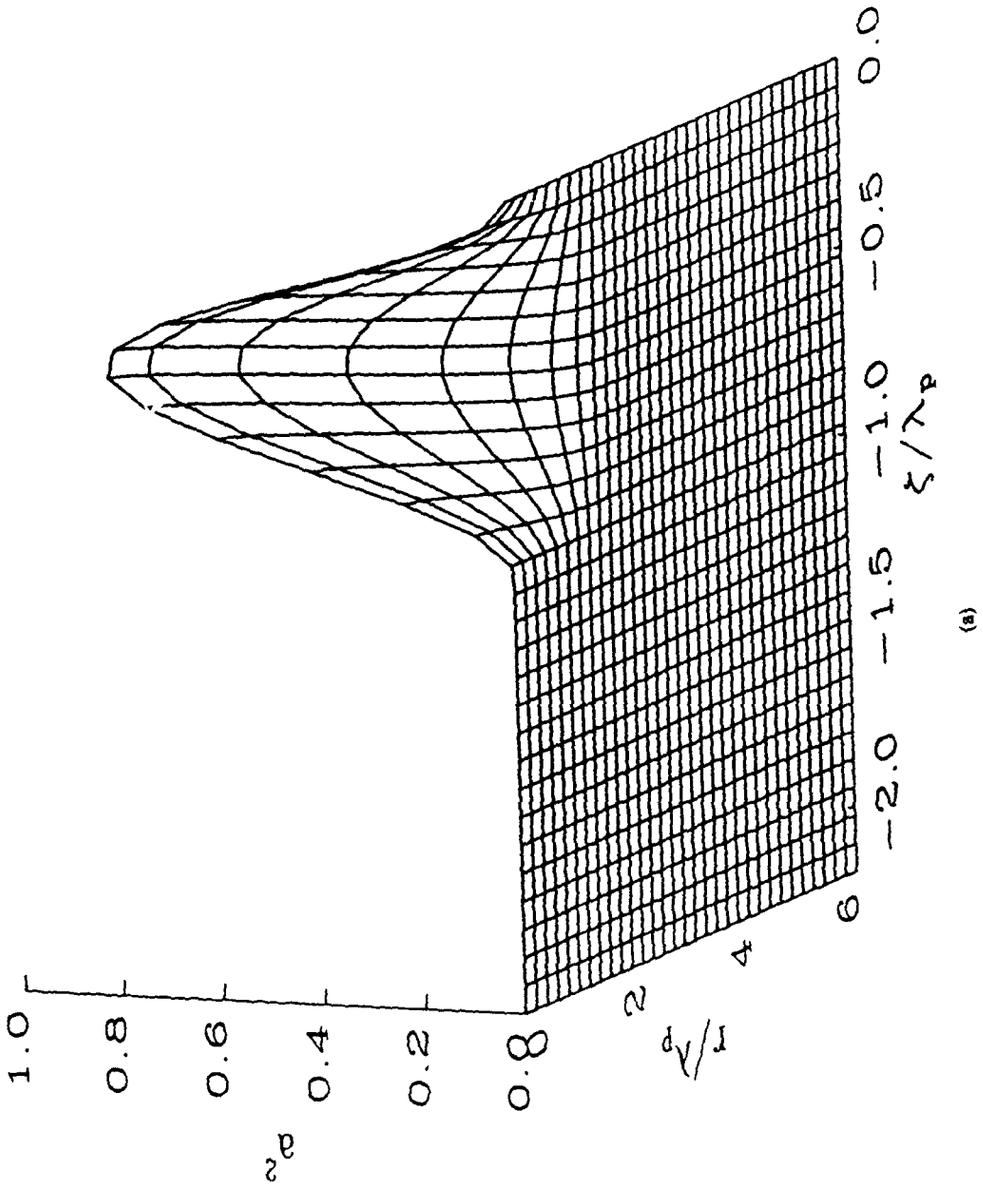

(a)

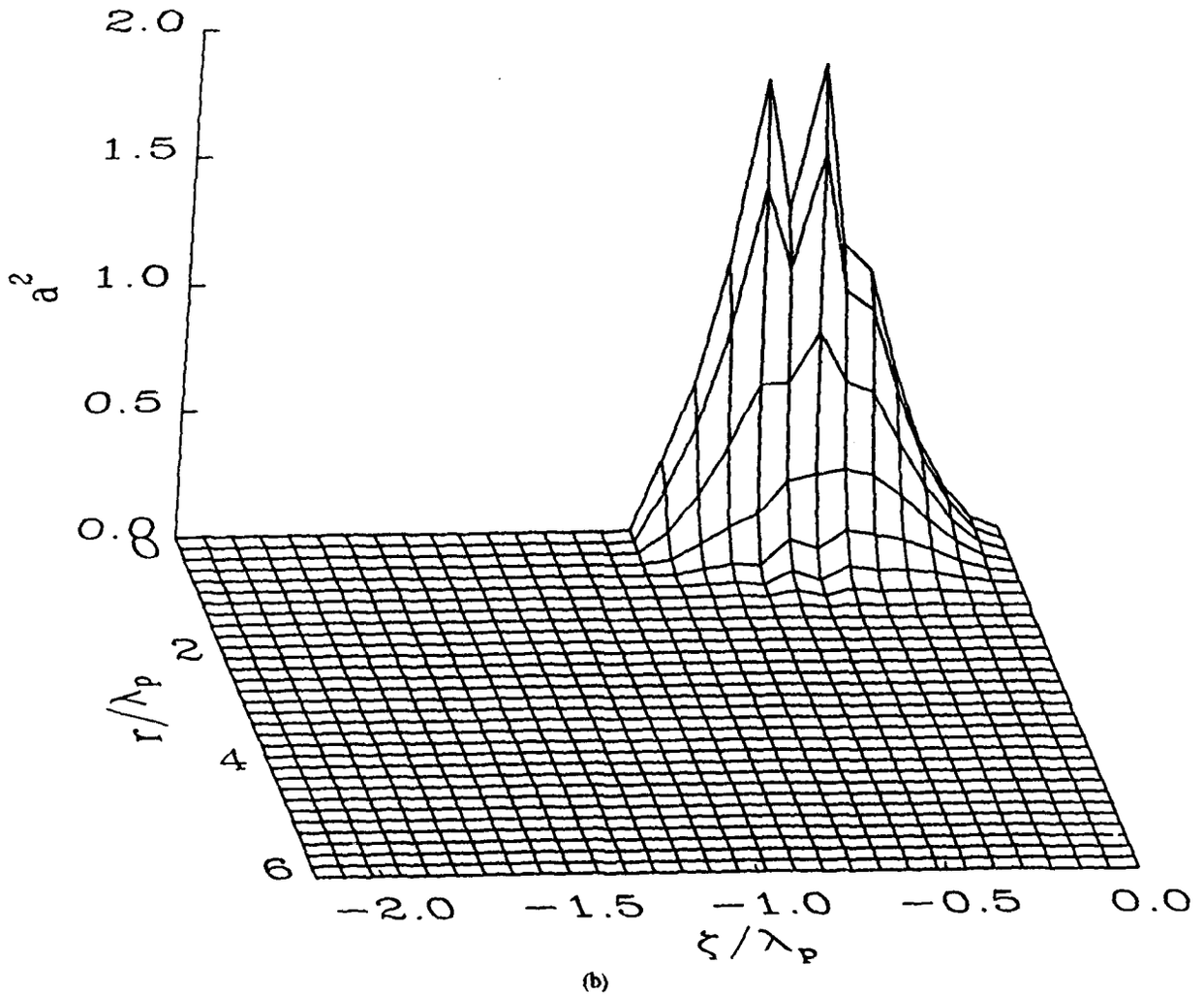

(b)

Fig. 5: The self-consistent propagation of an intense laser pulse, with $a_0 = 0.9$, $\lambda_0 = 1$ μm, and $c\tau_L = r_0 = \lambda_p = 0.03$ cm, in a density channel with $n(r = 0) = 1.2 \times 10^{16}$ cm^{-3}. (a) shows the initial normalized intensity profile, a^2. (b) shows the a^2 profile after propagating $10Z_R$, where $Z_R = 28.3$ cm.

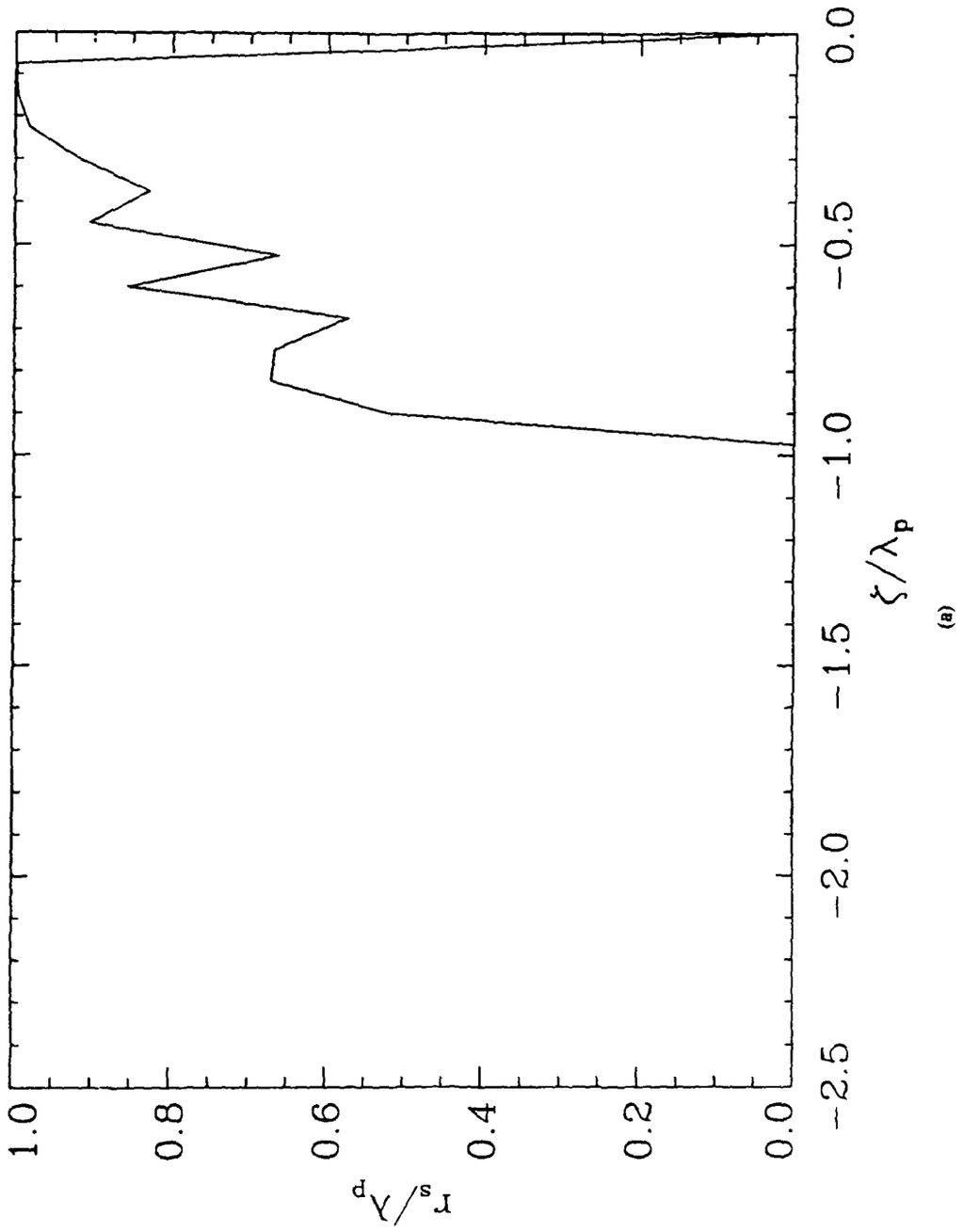
1.0
0.8
0.6
0.4
0.2
0.0
r_s/λ_p
0.0
−0.5
−1.0
−1.5
−2.0
−2.5
ζ/λ_p
(a)

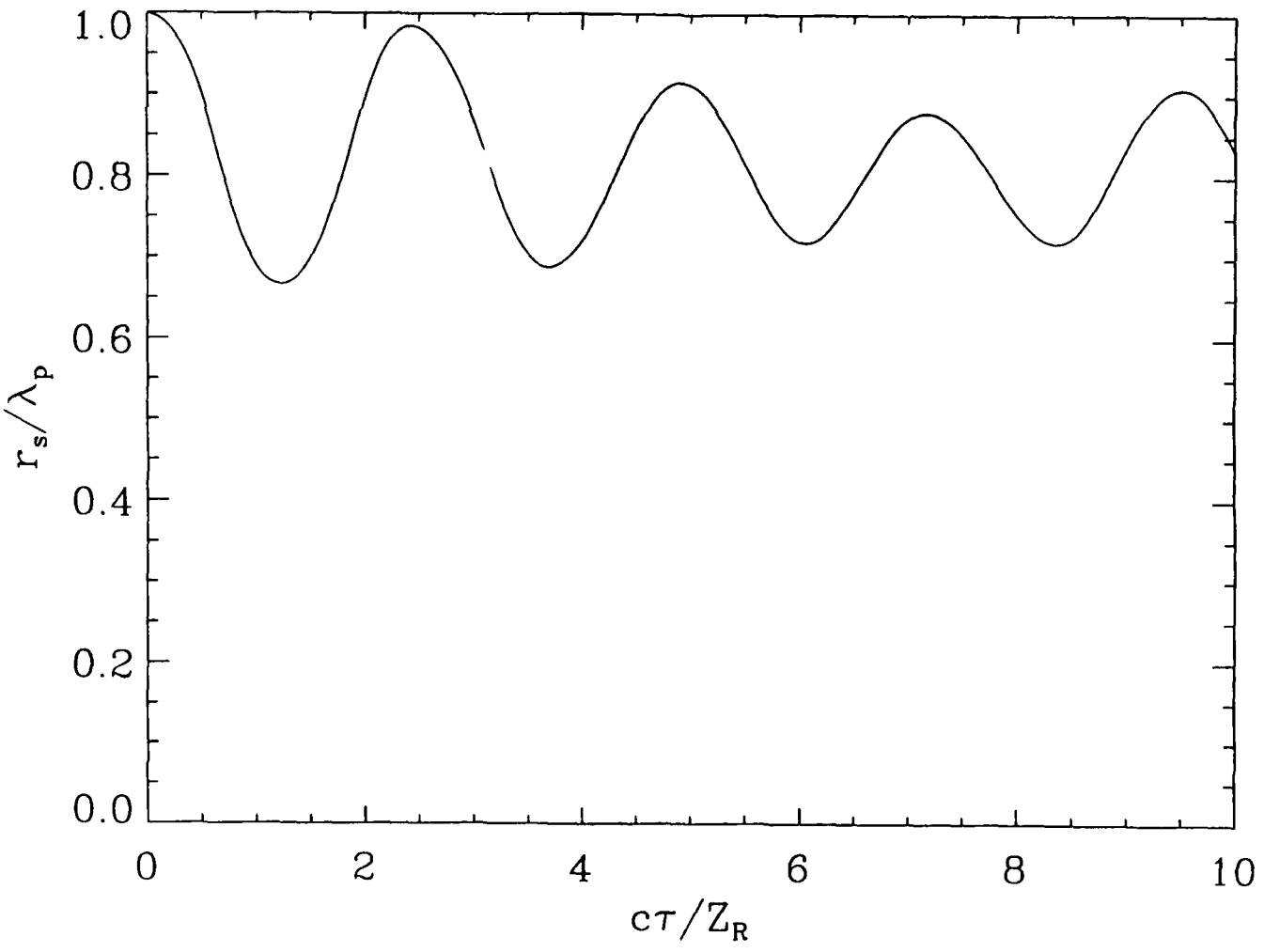

(b)

Fig. 6: The self-consistent propagation of an intense laser pulse in a plasma channel with same parameters as for Fig. 5. (a) shows the laser pulse spot size after $10Z_R$. (b) shows the behavior of the spot size at the pulse center as a function of propagation distance.

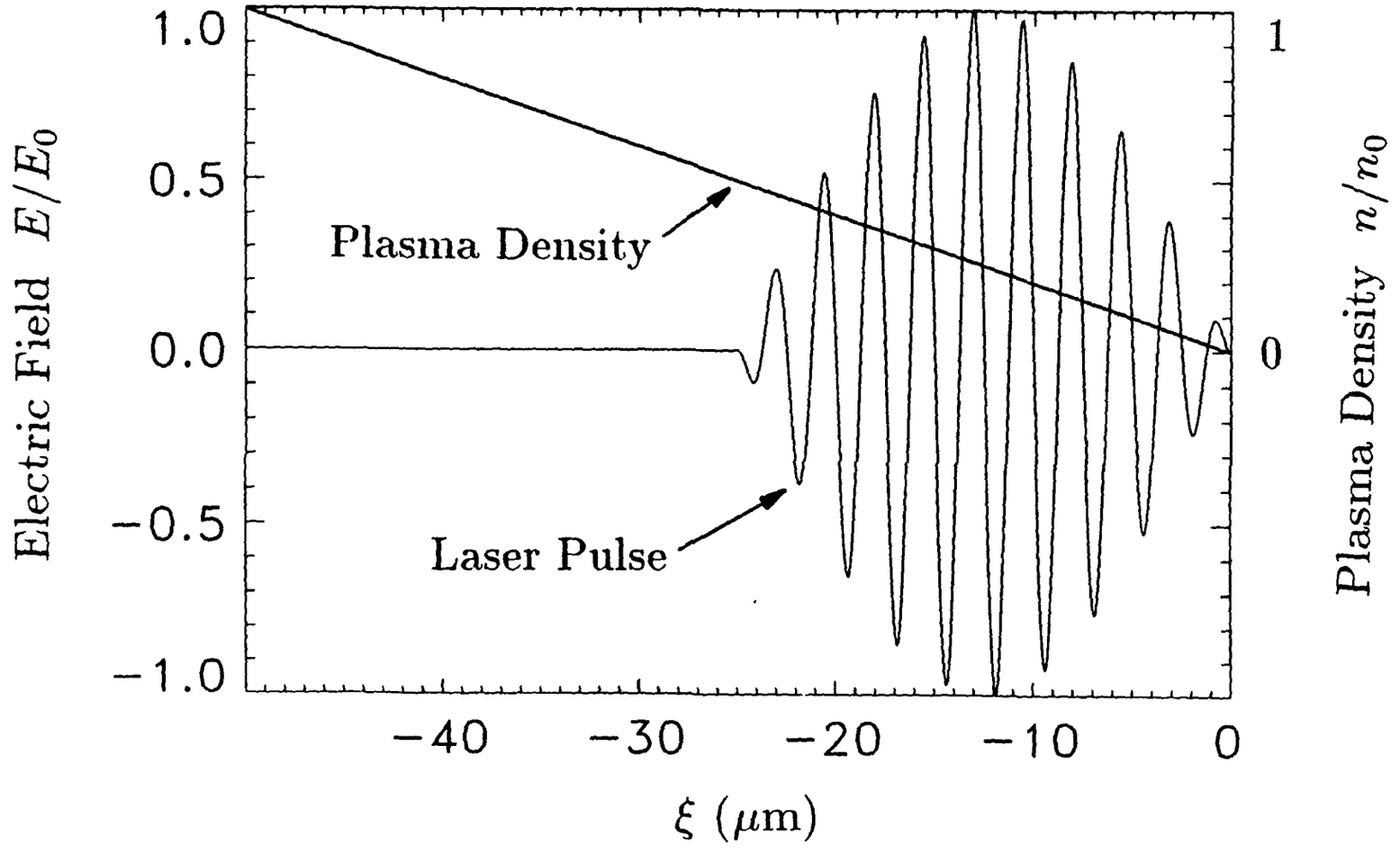
1.0
0.5
0.0
−0.5
−1.0
Electric Field E/E_0
Plasma Density
Laser Pulse
−40
−30
−20
−10
0
ξ (μm)
1
0
Plasma Density n/n_0

(a)

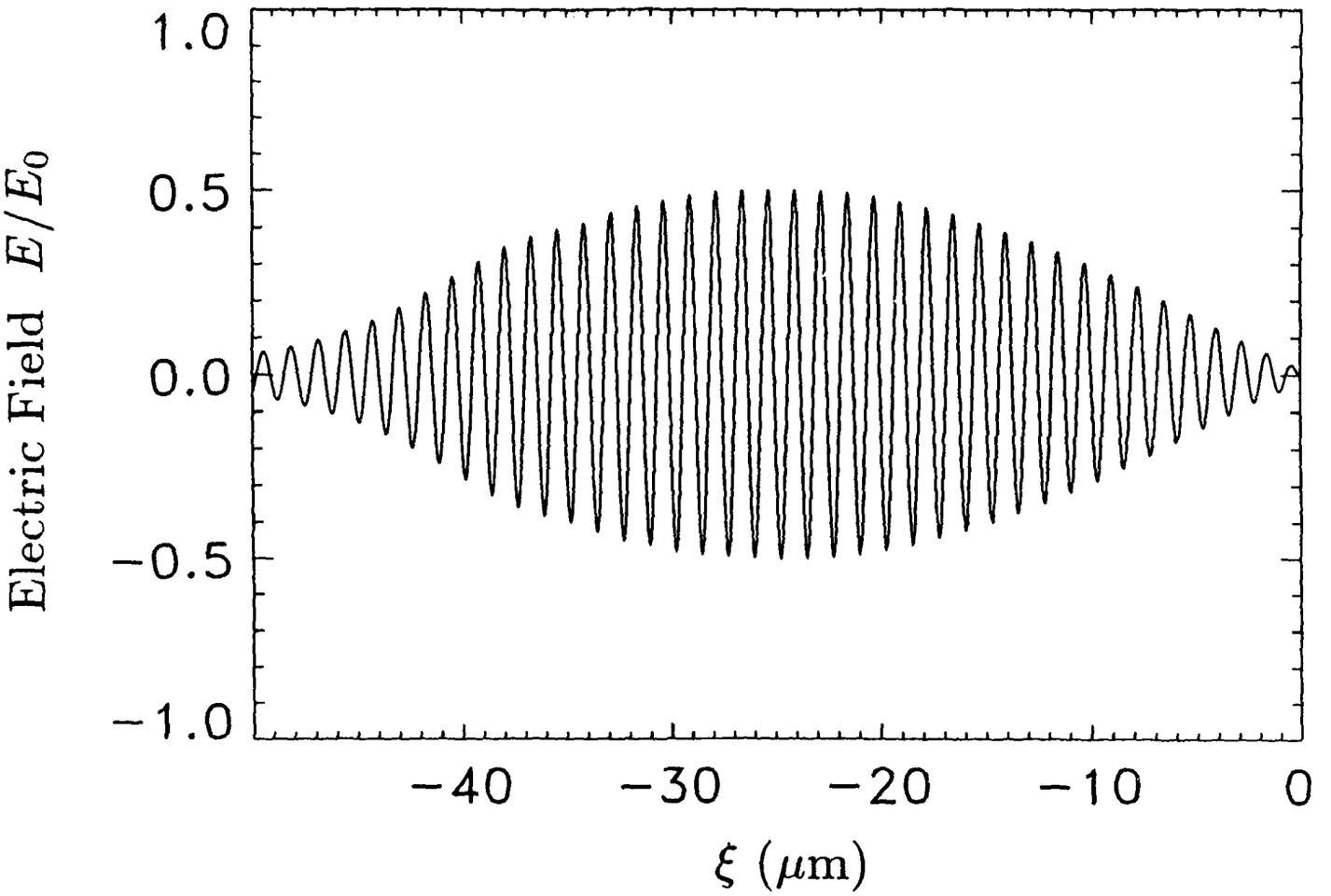

(b)

Fig. 7: The initial laser pulse and ionization density are shown in (a) as a function of $\xi = z - ct$. (b) shows the laser pulse after propagating the distance required for frequency doubling, as obtained from numerically solving the 1D wave equation.

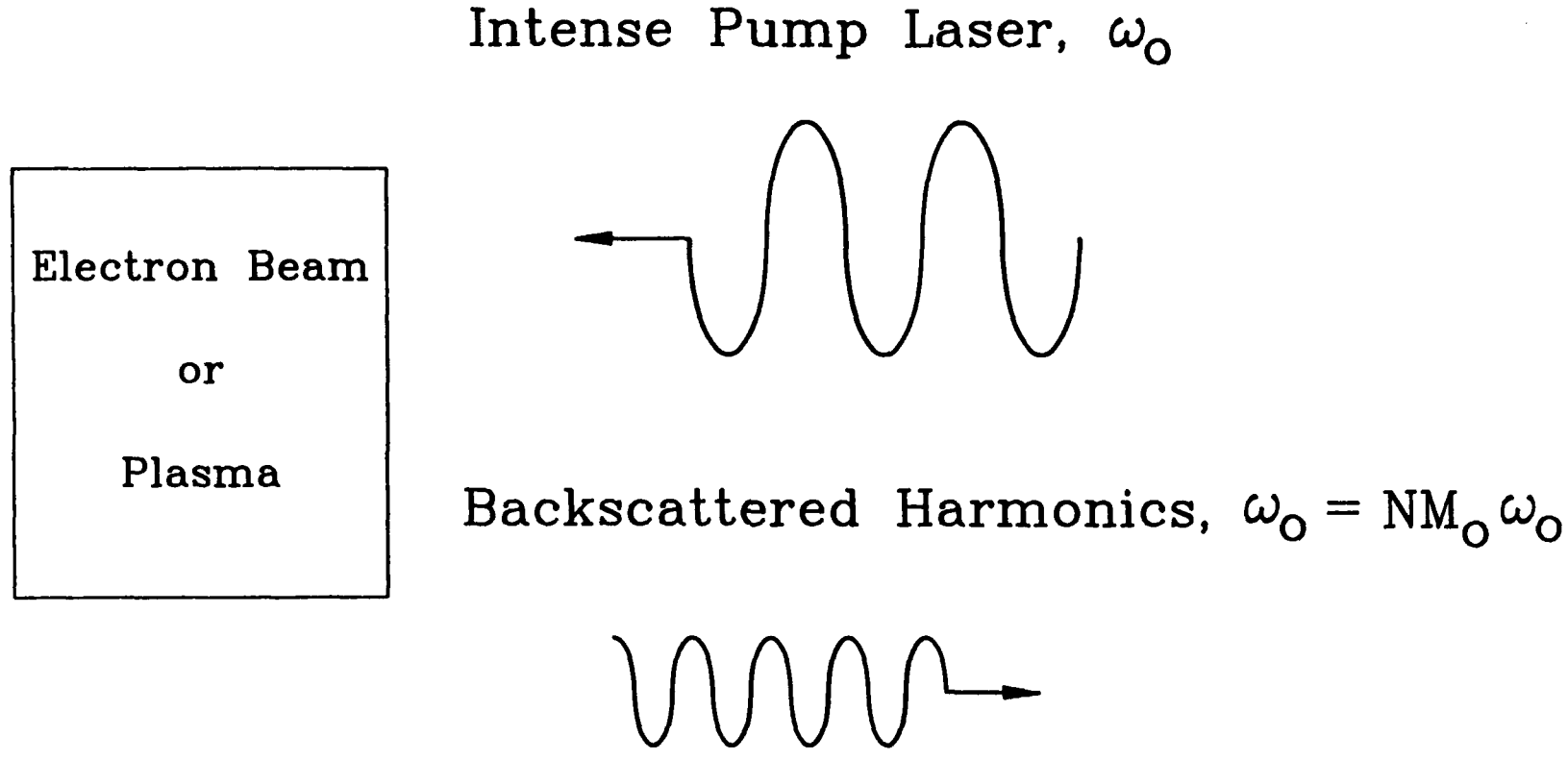

Fig. 8: Schematic of an intense laser of frequency ω_0 producing stimulated backscattered harmonic radiation from a plasma or a counterstreaming electron beam. The frequency of the backscattered radiation is $\omega = NM_0\omega_0$, where M_0 is the frequency Doppler shift factor, and $N = 1, 3, 5...$ is the harmonic number.

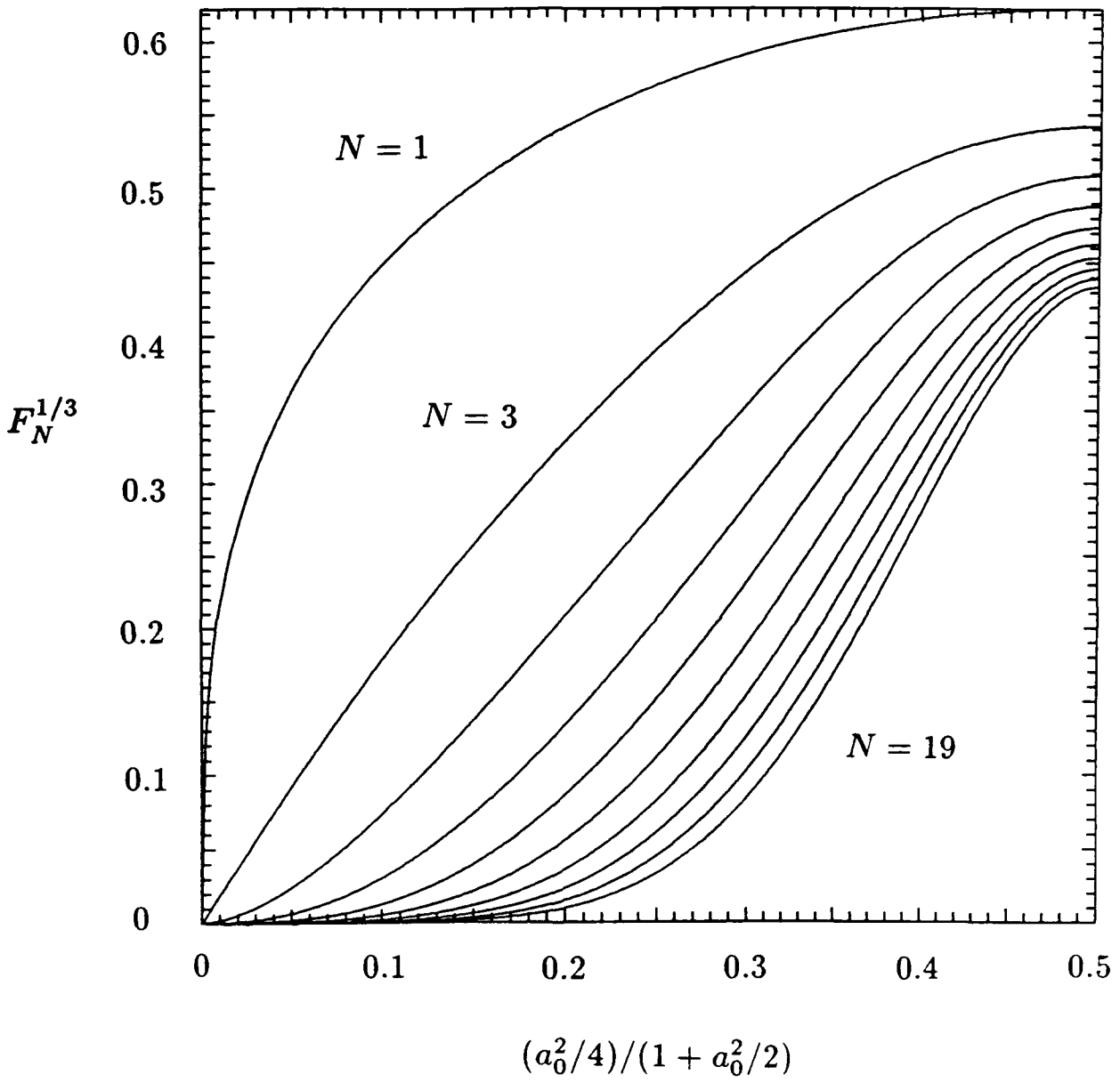

Fig. 9: The function $F_N^{1/3}$, proportional to the growth rate of the SBH radiation, verses the parameter $(a_0^2/4)/(1 + a_0^2/2)$.

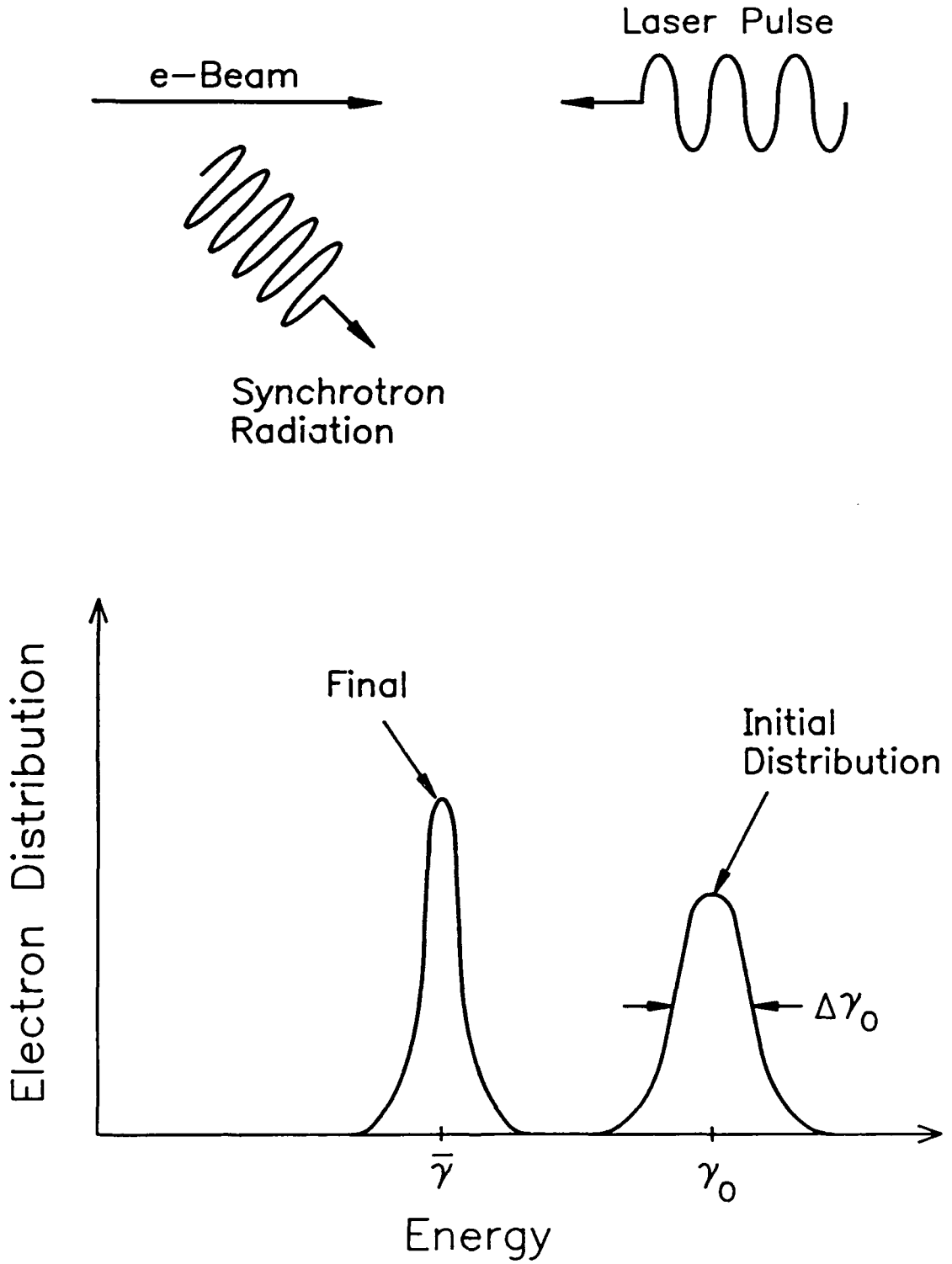

Fig. 10: Schematic of an intense laser interacting with a counterstreaming electron beam producing incoherent Thomson scattered radiation which leads to radiative cooling of the electron beam.